Lee Teng Internship: Argonne National Laboratory

Characterization of a mirror gimbal assembly for in-situ interferometric testing

Cassandra Phillips,[1,2*] Jon Montgomery,[1] Jun Qian,[1] Kurt Geotze,[1] Scott Izzo,[1] Sunil Bean,[1] Ray Conley,[1] and Lahsen Assoufid[1]

[1]*X-Ray Science Division, Argonne National Laboratory, 9700 S. Cass Avenue, Lemont, IL 60439, USA*
[2]*Washington State University, Pullman, WA 99164, USA*

Abstract

The modular deposition system (MDS) at the Advanced Photon Source (APS) located at Argonne National Laboratory is used to develop and fabricate advanced thin-film-based x-ray optics. The system has been designed primarily for multilayer deposition; however, it can accommodate several other capabilities to develop new fabrication techniques. One of these is the potential to integrate x-ray mirror surface figure correction techniques that require an ultra-high vacuum (UHV) processing environment with precision in-situ surface figure metrology. Metrology measurements are customarily done ex-situ with a separate metrology station in a controlled atmospheric environment. Coupling the two would significantly increase the iteration speed between cycles of surface figure measurement and correction, as well as potentially reduce mirror placement and registration errors. Here, Fizeau interferometry is employed outside the vacuum chamber, and the short-coherence source within the interferometer enables selection of individual optical paths within the interferogram. This design allows placement of the reference transmission optic (in our case, a λ/40 flat) inside the vacuum chamber, directly in plane with the surface under test (SUT). A UHV-compatible gimbal was designed and fabricated to both aim the reference flat with the SUT and rotate the reference flat in order to aid in systematic errors correction. The gimbal motion system is controlled using the Experimental Physics and Industrial Control System (EPICS). This work focuses on the control, characterization, and calibration of the gimbal actuation system as well as its testing using the Fizeau interferometer and reference transmission optics.

[*] Lee Teng Fellow at Argonne, June-August, 2019

Introduction

The modular deposition system (MDS, Figure 1) was built by the Advanced Photon Source (APS) at Argonne National Laboratory for the fabrication of advanced thin-film-based x-ray optics [1], including single-layer optics, multilayer optics, and graded multilayer optics. It was also designed to accommodate instrumentation and development efforts such as in-situ metrology, ion beam surface processing and correction, and multi-gas reactive sputtering for mirrors and substrates up to 1.4 meters long. Precision velocity profiling of the mirror is central to many of these techniques, such as differential deposition or producing lateral multilayer thickness gradients [2].

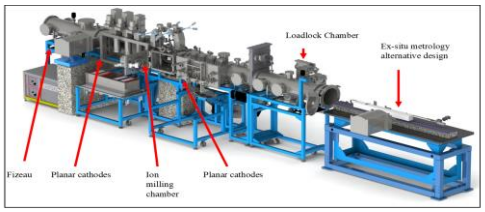

Figure 1: 3-D drawing of the modular deposition system.

The in-situ metrology design includes a high-speed, short-coherence dynamic interferometer (Figure 2), which is attached to the MDS (Figure 1). The reference optic is mounted on a high-precision motorized gimbal system (Figure 3), which, in the future, will reside within the vacuum chamber. An in-house-designed iris will isolate the reference mirror (here referred to as a transmission flat or TF) during the sputtering process. The gimbal allows the operator to accomplish two tasks with the TF while under vacuum: to rotate it for initial TF surface figure error mapping and tip/tilt it for alignment to the optical plane of the SUT [3].

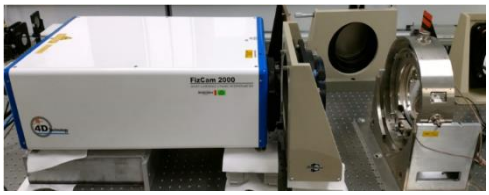

Figure 2: 4D Technology FizCam 2000 (left), and the gimbal assembly (right).

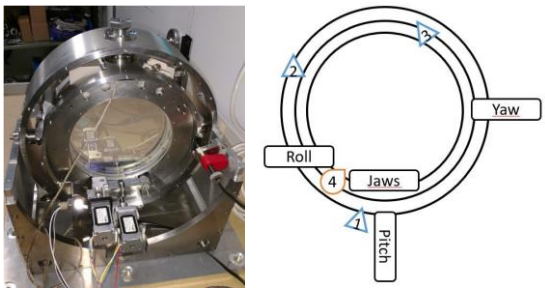

Figure 3: Photograph and schematic of the gimbal assembly.

The gimbal has four motors to incorporate three different motions —pitch (tilt along the horizontal axis), yaw (twist along vertical axis), and roll— and the jaws that elevate the TF off of the support band to roll (Figure 3). Roll is the innermost system, with the roll motion for the optic being engaged and disengaged by the jaws. The yaw controls the next ring, and the pitch controls the outer ring, tilting the entire system. The position of the pitch, yaw, and roll are measured by absolute encoders (Figure 3): The pitch encoder is at position 1, the yaw encoder at position 2, and the roll encoder at position 3. The absolute encoders allow for precision motion independent of errors inherent in mechanical systems and provide excellent long-term positional stability.

The transmission flat is supported during measurements by a steel band to mitigate point pressure distortions in the TF. In order to roll the TF, the jaws draw two sets of roll wheels together, which elevates the TF off the band and onto the wheels. In order to disengage the TF after rolling, the jaws separate, dropping the TF back onto the band. It can no longer roll but can still be manipulated using the pitch and yaw. A Hall sensor (position 4) is triggered when the jaws are fully open, and the roll is disengaged. The lower gap limit for the jaws is 6 mm, and the upper limit is 25 mm. The roll can be engaged when the jaws are at 11 mm or less with negligible slippage.

There are two types of motors used in the gimbal apparatus: piezo-based pico-motors from Newport Corporation, and stepper motors. The pitch and yaw utilize pico-motors, while the roll and jaws use stepper motors. The stepper motors have no intrinsic slippage, and while the jaw apparatus is gear-driven, the roll wheels are friction-based and must be fully engaged to rotate clockwise in order to minimize slippage. The pico-motor step size is nonlinear and also

dependent on load, which is discussed in further detail below.

Setup and Measurement

The project detailed in this paper was to calibrate the motion axes and test the gimbal for use in the MDS. The pico-motors and stepper motors were integrated with EPICS before testing the gimbal's mechanical performance. This task involved calibrating engineering units for the motor steps and determining potential issues with backlash and slippage for each axis. Finally, positional feedback was decoupled from motor steps and made dependent on feedback from the absolute encoders mounted along all three axes. Repeatability, precision, and communication between the axes of motion were tested for pitch, yaw, and roll. The jaws were also tested for slippage or backlash. For interferometry testing, the FizCam2000 was used to check the calibrations and provide more precise results for repeatability.

Gimbal Characterization

To provide position feedback, Renishaw Resolute UHV absolute encoders were wrapped around the transmission flat as well as along partial arcs following both pointing axes. The encoder's linear resolution was verified first and converted to angular motion. Table 1 shows the information gathered as well as the minimum and maximum angles of motion. The encoder strip along the circumference of the optic, used for the roll's encoder, meets with a small joint, and the encoder is not able to obtain a signal at that position. The angle that is unmeasurable is about 1.2°, which is why the roll has a minimum and maximum angle.

Table 1: Parameters for EPICS integration and angle limits.

Motor	nm/count	nrad/count
Pitch	1	7.86
Yaw	1	9.69
Roll	1	12.34
Motor	**Min Angle**	**Max Angle**
Pitch	-1.8°	2.67°
Yaw	-5.5°	2.8°
Roll	0°	358.83°

Since the picomotors, which are asymmetrically loaded along their motion axis, are piezo-motor driven, each motor has a different and asymmetric step size depending on direction. This was measured as a preferential slippage along some distance of travel. Figure 4 shows the slippage for pitch, yaw, and roll. For pitch, the least amount of slippage was at a velocity of 500 motor steps/sec and the average slippage for that speed was 0.15 mm per 2.257e5 encoder counts (0.1°).

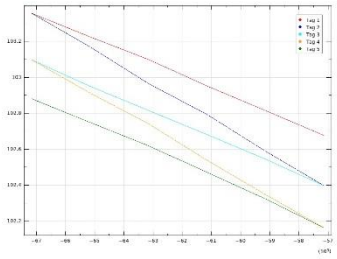

Figure 4: Pitch scan at speeds: 500, 1000, 1500, and 2000 steps/sec.

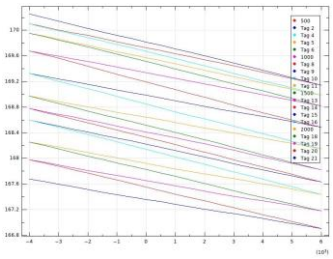

Figure 5: Yaw slippage scan

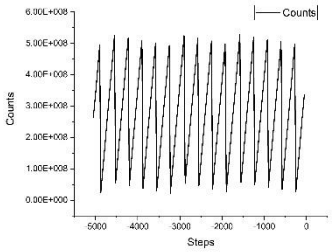

Figure 6: Roll test for repeatability and slippage analysis

The smallest amount of slippage was recorded for yaw at a velocity of 1500 steps per second. It was observed that over repeated motion, there was a decrease in directional slippage. The average measured slippage for the yaw encoder was 0.249 mm for 4.907×10^5 encoder counts (0.27°), as shown in Figure 5. The same test was done for pitch, which had an average measured slippage of 0.227 mm for 500 steps of negative and positive motion.

Figure 6 shows the repeatability of roll, as the jaws were at a 9.5 mm separation distance and will have minimal slippage. Since a scan is defined in discrete steps, there will always be

some travel due to variable slippage. This can be seen in Figure 6 above.

The stability of pitch, yaw, and roll was found through two scanning sequences using the angles calculated from the encoders: one every second for 100 seconds, and one every four hours for 60 hours. The 100-second scan is shown in Figure 7. The 60-hour scan is shown in Figure 8.

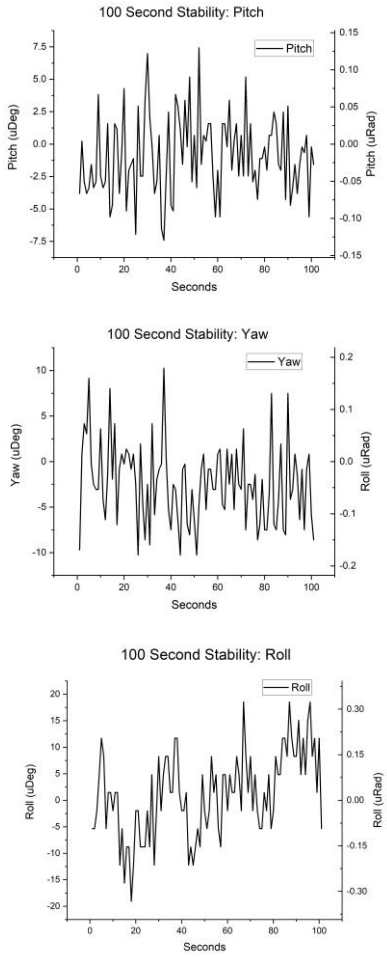

Figure 7: Data measured over 100 seconds.

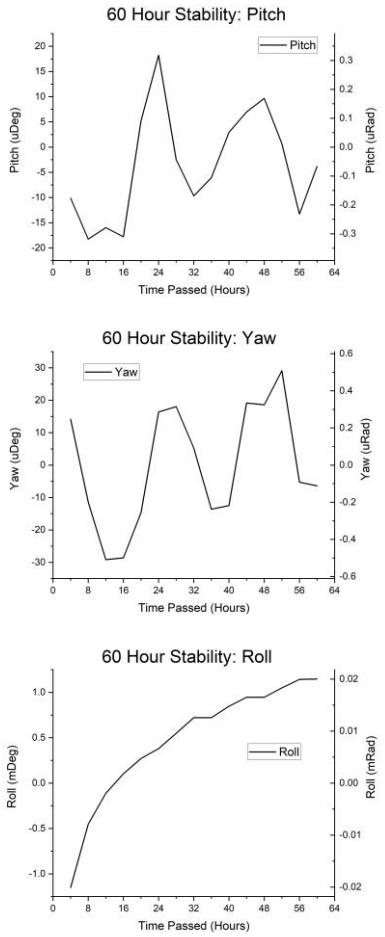

Figure 8: Data measured over one weekend.

For the 100-second scan, the pitch only deviated by 0.2593 µrad, and the yaw deviated by 0.3585 µrad. The roll changed more (0.656 µrad) because of its dependence on the wheels and the band. This is can be seen in the roll graph in Figure 7. Over 60 hours, the pitch still only changed by 0.6364 µrad, and the yaw changed by 1.0175 µrad.

The roll, however, changed 40.11 µrad over the 60 hours. This demonstrates that the gimbal is stable within the acceptable range and can be used to house the reference optic for metrology within the deposition chamber.

To test the system stability, one motor was moved, and the encoders for the other motors were interrogated to check whether there was any movement after the motor stopped. The pitch and yaw were moved from 0° to 0.05° in steps of 0.005°. For each movement step, the the encoder is sampled 60 times to reduce noise. The average RMS values and standard deviation are seen in Table 2. There is little correlation between movements. However, the standard deviation between the RMS values found in each of the eleven scans for each test

is sufficiently small that its effects can be disregarded.

RMS average and standard deviation values Move	Measure	RMS Avg	StdDev
Pitch	Roll (µrad)	0.93031	2.06E-07
Pitch	Yaw (µrad)	0.3085	0.0734
Yaw	Pitch (µrad)	0.08502	0.05699
Yaw	Roll (µrad)	0.93032	1.88E-07

Finally, the jaws' repeatability was tested. The interference pattern from the FizCam2000 was centered, and the pitch and yaw angle noted. The jaws were moved from 1000 motor steps to 15,000 steps and back. Once repositioned to the center, the pitch and yaw angles were noted again. The difference between one noted angle and the next was graphed, as seen in Figure 9. The interference pattern never returned to the original position.

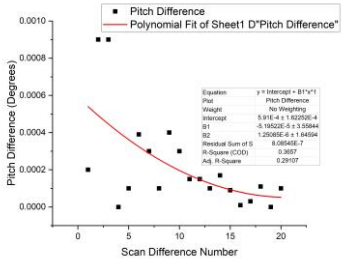

(a) Pitch analysis

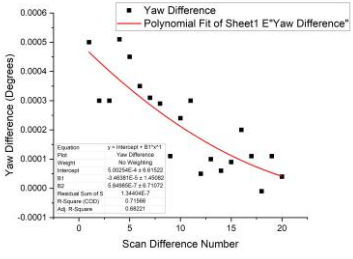

(b) Yaw analysis

Figure 9: Data collected and analyzed for testing jaw repeatability.

As can be seen, the movement needed to re-center the interference pattern decreased the more times the jaws were opened and shut. This result shows that the TF will never return to exactly the same place, and the operator must re-center the TF after roll operations (as expected). However, the jaw action can be repetitively cycled to improve its repeatability.

Overall, gimbal stability was within 0.636 µrad along the pitch axis, 1.018 µrad along the yaw axis, and 40.11 µrad along the roll axis over 60 hours, but 0.259 µrad for the pitch, 0.359 µrad for the yaw, and 0.656 µrad for the roll over a 100-second period. The ringing is also negligible, showing that there is little correlation between the movement of one motor and an undesired movement in another direction. The analysis shows that the movements are repeatable and that the gimbal is calibrated.

Optical Measurements

Using the 4D Technology FizCam2000, three optics were measured to compare the stability of two stationary transmission flats the gimbal. The measurements for two stationary transmission flats and the gimbal optic to be used as a reference optic in the MDS can be seen in Figure 10. The peak-to-valley ratio (PVR) for the gimbal optic was 19.7 nm. Transmission flat 1's PVR was only 24.3 nm, and transmission flat 2's was 31.2 nm; therefore, the TF mounted in the gimbal is the flattest optic out of the three. It is convenient to already have the flattest TF mounted inside the gimbal for future use. It was also apparent that the gimbal is sufficiently stable to allow accurate and precise measurements with the interferometer.

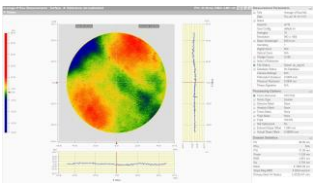

(a) Transmission flat 1 (stationary)

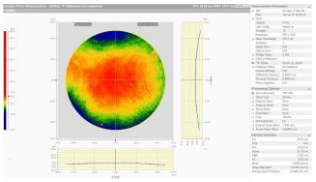

(b) Transmission flat 2 (stationary)

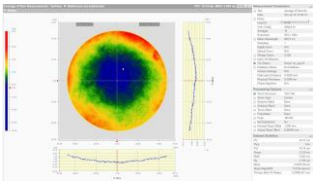

(c) Transmission flat 3 (mounted in gimbal)

Figure 10: Measurements for three transmission flats.

The angular calibration of the gimbal was checked using the interferometer by slightly changing the angle of one axis (which is feedback-controlled by the absolute encoders) and taking a corresponding interferometry measurement. The results, comparing the angle changes between the encoder calculated measurements and the interferometer measurements, are shown in Figure 11. A linear correlation very close to 1 was observed for every data set, indicating excellent linearity across the entire range of travel for both axes.

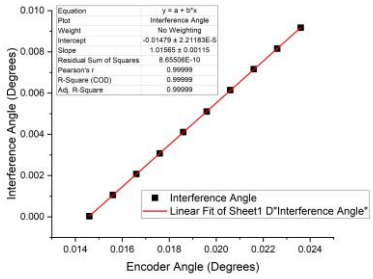

(a) Pitch motion in the positive direction

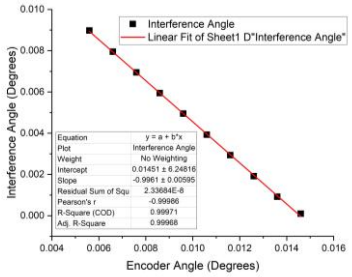

(b) Pitch motion in the negative direction

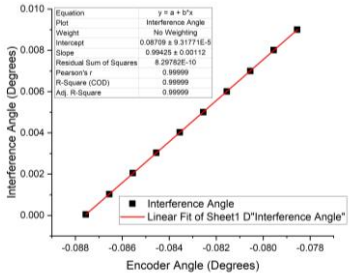

(c) Yaw motion in the positive direction

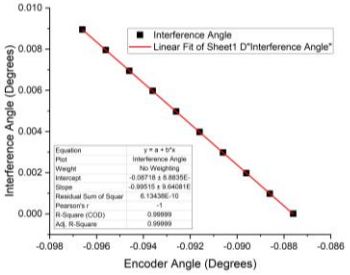

(d) Yaw motion in the negative direction

Figure 11: Angle analysis for encoder measurement versus interferometry measurement.

Figure 12 illustrates the sensitivity of the interference pattern to minor pointing angle adjustments to the gimbal axes. This set of six patterns also demonstrates the repeatability of each axis. For each, the interference center was found, and one motor was changed by 0.001° and then returned to the previous position of the encoder. The resulting interference patterns are below.

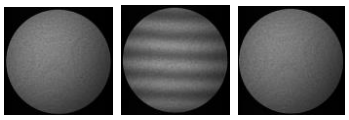

(a) Changing pitch

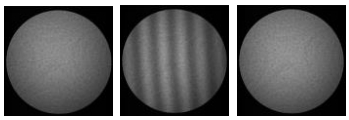

(b) Changing yaw

Figure 12: Interference patterns when one motor moves 0.001° in the positive direction from the interference center and back.

Pitch and yaw are very repeatable, given the interference patterns. This repeatability was measured by (1) taking a reference interferometry measurement, (2) inducing an angular change in the TF with the gimbal, (3) going back to the starting position, and (4) taking another interferometry reference for subtraction from the measurement in step 1. The angle difference between the two measurements gives the angle slippage. That was done ten times for both the pitch and the yaw, readjusting to the center of the interference pattern between each set of measurements. This was done for 0.001° for both and then 0.005° for the pitch to see if larger angles have coarser angular displacement. The results are shown in Table 3.

Table 3: Average angular differences.

Motor$_{axis}$ (move)	**Avg angle Diff**	**STDDEV**
Pitch$_X$ (0.001°)	1.608E-7°	9.127E-8°
Pitch$_Y$ (0.001°)	3.792E-7°	7.466E-7°
Pitch$_X$ (0.005°)	8.139E-8°	5.529E-8°
Pitch$_Y$ (0.005°)	1.391E-7°	1.520E-7°
Yaw$_X$ (0.001°)	1.249E-7°	6.986E-8°
Yaw$_Y$ (0.001°)	1.414E-7°	8.235E-8°

Conclusion and future work

The angular deviation between axis movements when measured with the gimbal encoders versus the interferometer is within the 10^{-7} degree (~10 nanoradians) range for pitch and yaw, indicating that if active pointing control is enabled (using the gimbal encoders), the instrument will perform well within the starting parameter space and be useable for in-situ optical metrology. The data collected for the mechanical analysis shows that the passive system stability (when powered off) settles to within 700 nanoradians. The channel access Qt display manager (CaQtDM) HMI is ready to integrate into the MDS control structure. The above results indicate that the gimbal is functioning adequately and is ready to be placed into the vacuum system of the deposition chamber and used.

The optical measurements illustrate that the gimbal is capable of precisely centering on the surface under test, its motion is linear, and its angular alignment agrees well with the interferometer. Although roll is not intended to be a precise motion, the desired analyses for this axis were not able to be completed within the scope of this work.

Acknowledgments

I would like to thank Dr. Lahsen Assoufid for mentoring me throughout the project, Dr. Raymond Conley and Jon Montgomery for providing guidance for the gimbal measurements, Jun Qian for help with interferometry, and the Lee Teng Internship for this opportunity.

*The research at Argonne National Laboratory was supported by the U.S. Department of Energy Office of Science-Basic Energy Sciences under Contract No. DE-AC-02–06CH11357.

References

[1] Als-Nielsen, J., and D. McMorrow. 2011. *Elements of Modern X-Ray Physics*. Rochester, NY: Wiley.

[2] Conley, R., Shi, B., Erdmann, M., Izzo, S, Assoufid, L., Goetze, K., Mooney T., Lauer, K. 2014. "APS deposition facility upgrades and future plans," Proc. SPIE 9207, Advances in X-Ray/EUV Optics and Components IX, 92070I (5 September 2014).

[3] Conley, R., Qian, J., Erdmann, M., Kasman, E., Assoufid, L., Izzo, S. 2018. Precision Surface Measurement in a Vacuum. US Patent # 10,151,574, filed July 12, 2017 and issued Dec. 11, 2018.